

# APPLICATION OF COMPOSITE POLYMER ELECTROLYTES

Principal investigator:

Prof. Bruno Scrosati  
Department of Chemistry  
University of Rome "La Sapienza"  
Piazza Aldo Moro 5, 00185 Rome, Italy

CONTRACT NUMBER: N68171-00-M-5848

FINAL REPORT  
*May 2001*

8931 CH 01

The research reported in this document has been made possible through the support and the sponsorship of the U.S. Government through its European Research Office of the U.S. Army.

**DISTRIBUTION STATEMENT A**  
Approved for Public Release  
Distribution Unlimited

20010827 066

## Summary of the scientific work done during the project period

In this project we have first refined the model to account for the role of the ceramic fillers in enhancing the transport and the interfacial properties of poly(ethylene oxide)PEO-based composite polymer electrolytes, by a series of specifically addressed electrochemical tests which included the determination of the conductivity and of the lithium transference number of various composite electrolyte samples only differing from the type of the surface states of the ceramic filler. The results were described in details in the 1<sup>st</sup> Interim Report.

Our following task was that of completing the investigation of the nanocomposite polymer electrolytes formed by dispersing 10 w/o  $\text{Al}_2\text{O}_3$  basic, neutral or acidic, respectively, ceramic filler in a  $\text{P(EO)}_{20}\text{LiCF}_3\text{SO}_3$  matrix, in view of their use as improved separators in novel types of lithium rechargeable batteries. The investigation was directed to the determination of the electrochemical stability window and of the interfacial characteristics of the lithium electrode. The results were reported in the 2<sup>nd</sup> Interim Report.

Finally, we have characterized a Li-insertion compound of  $\text{LiMn}_3\text{O}_6$  formula, with the aim of evaluating its potentiality as cathode material in prototypes of the above mentioned lithium rechargeable batteries. This part of the work was described in the 3<sup>rd</sup> Interim report.

In this final report we summarize the most significant results of this work. These results have been at various conferences, such as the "7<sup>th</sup> International Symposium on Polymer Electrolytes", ISPE-7, Noosa, Australia, August 2000 and the 5<sup>th</sup> Tapei Battery Forum, Taipei, Taiwan, April 2001.

In addition they have been the object of the following two publications:

- 1) F. Croce, L. Persi, B. Scrosati, F. Serraino-Fiory, E. Plichta, M.A. Hendrickson, "Role of the ceramic fillers in enhancing the transport properties of composite polymer electrolytes" *Electrochimica Acta*, in press.
- 2) L. Persi, B. Scrosati, E. Plichta, M.A. Hendrickson, "Poly(ethylene oxide), nano-composite electrolytes as improved separators for rechargeable lithium polymer batteries. The Li-  $\text{LiMn}_3\text{O}_6$  case" submitted to *J. Electrochem. Soc.*

## 1. Synthesis of composite polymer electrolytes

The composite polymer electrolytes were obtained by combining poly(ethylene oxide) PEO with  $\text{LiCF}_3\text{SO}_3$  and using three forms of  $\text{Al}_2\text{O}_3$ , i.e., acidic, basic or neutral, respectively, as the ceramic filler. The  $\text{LiCF}_3\text{SO}_3$ /PEO concentration ratio was fixed to 1/20 and the amount of added ceramic to 10 % of the total  $\text{PEO}_{20}\text{-LiCF}_3\text{SO}_3$  weight. The preparation of the composite electrolyte samples involved first the dispersion of the selected ceramic powder and of the  $\text{LiCF}_3\text{SO}_3$  lithium salt in acetonitrile, followed by the addition of the PEO polymer component and by a thorough mixing of the resulting slurry. The slurry was then cast onto a teflon plate and the solvent allowed to evaporate slowly at room temperature by trapping it into molecular sieves. This procedure yielded homogenous and mechanically stable membranes of average thickness of 100  $\mu\text{m}$  which were dried under vacuum at 45-50°C for 24 hours.

## 2. Experimental techniques.

The characterization of the composite electrolytes was mainly carried out by electrochemical techniques. The lithium ion transference number,  $T_{\text{Li}^+}$ , was evaluated by sweep voltammetry combined with impedance spectroscopy, by first imposing a dc polarization pulse to a cell of the Li / electrolyte sample / Li type and by following the time evolution of the resulting current flow. The purpose was to measure the initial and the steady-state value of the current flowing through the cell during polarization. Impedance spectra were taken before and after the pulse application in order to correct for the change in impedance of the test cell during the experiment.

The electrochemical stability window was measured by running a sweep voltammetry of an "inert" (e.g., stainless steel) electrode in the given electrolyte sample. Under these conditions, the voltage at the onset of the current on the cathodic scan has been associated to the electrolyte brake-down voltage.

The characteristics of the composite polymer electrolyte/lithium metal electrode interface were investigated by monitoring the time evolution of the impedance of

cells formed by sandwiching the given electrolyte sample between two lithium electrodes.

The application of the preferred composite electrolyte, namely the  $\text{P(EO)}_{20}\text{LiCF}_3\text{SO}_3 + 10 \text{ w/o Al}_2\text{O}_3$  neutral membrane was tested by using it as separator of a lithium battery having a

Li-insertion cathode of  $\text{LiMn}_3\text{O}_6$  formula. We have found that the properties of this cathode material depend to a great extent from its synthesis procedure. Therefore, we have tested samples from different sources. One of this was provided by the US Army Research Laboratory in Fort Monmouth. Alternatively, also samples kindly provided Chunco Denki Koygo Co. LTD., Japan, have been used. In the case of the  $\text{LiMn}_3\text{O}_6$  Fort Monmouth samples, the electrodes were prepared in the form of blended films, by mixing the given  $\text{LiMn}_3\text{O}_6$  sample at a 82 weight percent, w/o, ratio with carbon (Super P, conductive component, 8 w/o) and PVdF (binder, 10 w/o). This mixture was dispersed in tetrahydrofuran, THF. The resulting slurry was spread on an aluminum foil current collector by evaporating off the residual THF and by hot-rolling. When using the  $\text{LiMn}_3\text{O}_6$  samples received from Chunco Denki Koygo, the film electrodes were prepared, by mixing the given  $\text{LiMn}_3\text{O}_6$  sample at a 80 weight percent, w/o, ratio with carbon (Super P, conductive component, 10 w/o) and PEO (binder, 10 w/o). Similarly to the previous case, a THF slurry of the mixture was cast on an aluminum foil current collector.

Both procedures gave thin film electrodes having good transport (high and uniform conductivity) and favorable mechanical (good plasticity and adhesion) properties. These  $\text{LiMn}_3\text{O}_6$  films were tested as cathodes in laminated battery prototypes having a lithium metal foil anode and a  $\text{P(EO)}_{20}\text{LiCF}_3\text{SO}_3 + 10 \text{ w/o Al}_2\text{O}_3$  composite membrane electrolyte. All the manipulations and the assemblage of the battery prototypes were carried out in a controlled-environment dry box. The battery characteristics and performance were determined by monitoring the charge-discharge cycles run and controlled by an automatic battery cycler. The testing temperature varied from 83 °C to 105 °C, according to the experimental conditions.

### 3. Model of transport mechanism in PEO-based composite polymer electrolytes.

As demonstrated in previous reports of former research contracts the conductivity of composite polymer electrolytes formed by dispersing in a PEO-LiX matrix nano-particle size ceramics (e.g,  $\text{TiO}_2$ ,  $\text{Al}_2\text{O}_3$  or  $\text{SiO}_2$ , respectively) is consistently higher (i.e. about two order of magnitudes at ambient temperature) than that of the corresponding ceramic-free polymer electrolytes. This has been explained assuming the occurrence of Lewis acid-base-type specific interactions between the surface groups of the ceramic particles and both the PEO segments and the lithium salt anions. These interactions induce local structural modifications due i) cross-linking centers for the PEO segments and for the  $\text{X}^-$  anions, this promoting preferential  $\text{Li}^+$  conducting pathways at the ceramics' surface and ii) Lewis acid-base interaction centers with the electrolyte ionic species, this promoting salt dissociation *via* a sort of "ion-ceramic complex" formation. The combined effect is the promotion of "free" ions and thus, this model may indeed account for the observed enhancement of the conductivity of the nanocomposites in a wide temperature range. In this project we have confirmed the model by carrying out *ad hoc* measurements, such as the determination of the transport properties of a series of composite electrolytes differing only from the types of the surface states of the ceramic filler. For this particular test we have selected the  $\text{P}(\text{EO})_{20}\text{LiSO}_3\text{CF}_3$  polymer matrix with the addition of 10 w/o  $\text{Al}_2\text{O}_3$ , this ceramic being available in three forms, i.e., acidic, basic and neutral, these in turn reflecting different surface group arrangements. The surface interactions are expected to vary according to the surface states of the ceramics. In the acidic the ceramic's surface OH groups are expected to favor interactions (via hydrogen bonding) with both the lithium salt anion and the PEO segments, with a consequent increase in salt dissociation and in the local PEO amorphous phase fraction; thus, enhancements in lithium ion transference number,  $T_{\text{Li}}^+$  and in ionic conductivity are expected. In the neutral case, due to the lower extent of the ceramic's surface groups, weaker interactions with both the lithium salt anion and the PEO segment are foreseen, with associated less important enhancements both in lithium ion transference number, and in ionic conductivity. Finally, in the case of basic  $\text{Al}_2\text{O}_3$  very few surface effects and thus, no macroscopic changes of ionic transport properties to respect to ceramic-free polymer electrolytes, are expected. In summary, the extent of structural

modifications induced by the ceramics should be increasing according to the following sequence  $\text{Al}_2\text{O}_3$  acidic >  $\text{Al}_2\text{O}_3$  neutral >  $\text{Al}_2\text{O}_3$  basic. This is in fact what has been found by comparing the Arrhenius conductivity plots of three  $\text{Al}_2\text{O}_3$ -based composite samples and, particularly the respective values of the lithium transference number. Table 1 shows that this parameter increases as much as 30% when passing from ceramic-free  $\text{P}(\text{EO})_{20}\text{LiCF}_3\text{SO}_3$  to composite  $\text{P}(\text{EO})_{20}\text{LiCF}_3\text{SO}_3$  formed by adding basic, neutral and acidic, respectively, filler. To be noted that an increase in  $\text{Li}^+$  ion transference number is particularly important in terms of applications in a practical lithium battery where the electrochemical mechanism is expected to be the insertion-deinsertion of the  $\text{Li}^+$  ions in selected intercalation cathodes. Under these conditions, the cell operation is solely controlled by the transport of the  $\text{Li}^+$  ions throughout the electrolyte, so that a high transference number results in low concentration polarizations, this in turn allowing high discharge rates, as indeed demonstrated in this project (see further on).

Table 1. Lithium transference number,  $T_+$ , at 95 °C of various composite  $\text{P}(\text{EO})_{20}\text{LiCF}_3\text{SO}_3$  nanocomposite polymer electrolyte samples determined from the impedance responses illustrated in Figure 5.

sample	$T_+$
$\text{P}(\text{EO})_{20}\text{LiCF}_3\text{SO}_3$ ceramic-free	0.46
$\text{P}(\text{EO})_{20}\text{LiCF}_3\text{SO}_3$ +10 % $\text{Al}_2\text{O}_3$ basic	0.48
$\text{P}(\text{EO})_{20}\text{LiCF}_3\text{SO}_3$ +10 % $\text{Al}_2\text{O}_3$ acid	0.54
$\text{P}(\text{EO})_{20}\text{LiCF}_3\text{SO}_3$ +10 % $\text{Al}_2\text{O}_3$ neutral.	0.63

#### 4. Electrolyte stability window

Figure 1 shows a typical voltammetric sweep run on a stainless steel electrode in a cell using a  $\text{P(EO)}_{20}\text{LiCF}_3\text{SO}_3$  +10 w/o  $\text{Al}_2\text{O}_3$  acid and basic, respectively, nanocomposite polymer electrolyte.

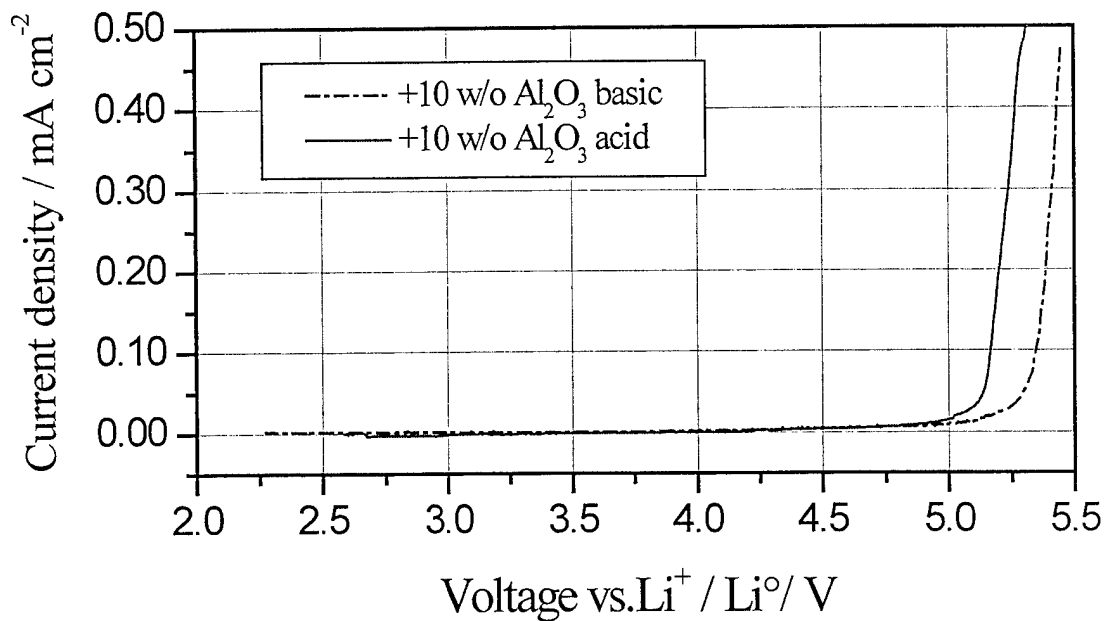


Figure 1. Current-voltage curve of a stainless-steel electrode in  $\text{P(EO)}_{20}\text{LiCF}_3\text{SO}_3$  +10 w/o  $\text{Al}_2\text{O}_3$  polymer electrolyte cells. Counter and reference electrode: Li.  $T=95^\circ\text{C}$ . Scan rate  $0.2\text{mV/s}$ .

The current onset is revealed around 5V vs. Li, and thus this value may be assumed as the brake-down voltage of the electrolytes. It has to be remarked, however, that the decomposition voltage determined by the test of Figure 1 is not thermodynamic but rather kinetic since depending on the nature of the working electrode. Thus, the decomposition value may vary passing from one testing electrode to another. Therefore, although apparently stable up to 5V vs. Li, the composite electrolyte may possibly decompose at lower voltage under different conditions. This suggests that a safe application of this electrolyte is in cells operating around the 4V level.

### Polymer electrolyte /lithium metal interface.

The behavior of the lithium electrode /  $\text{P(EO)}_{20}\text{LiCF}_3\text{SO}_3 + 10 \text{ w/o Al}_2\text{O}_3$  composite polymer electrolyte interface was investigated by impedance spectroscopy. The analysis of the impedance spectra by using fitting procedures based on appropriate equivalent circuit, has allowed to conclude that the interfacial resistance  $R_i$  is in fact the combination of the resistance associated to the passivation film growing on the lithium electrode surface  $R_f$ , and the charge-transfer resistance,  $R_{ct}$ .

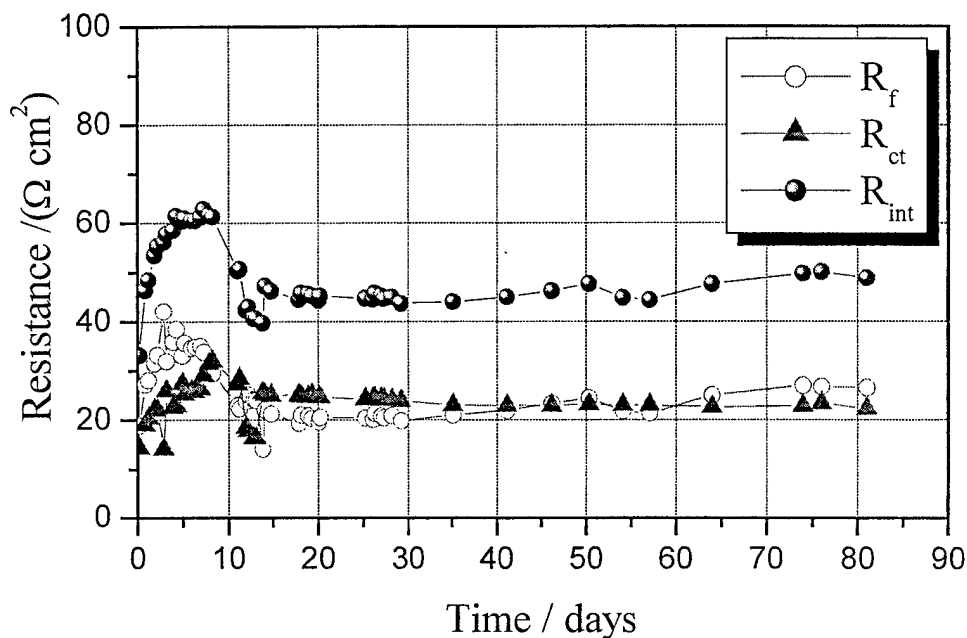


Figure 2. Time evolution of the resistance parameters of the  $\text{Li/P(EO)}_{20}\text{LiCF}_3\text{SO}_3 + 10 \text{ w/o Al}_2\text{O}_3$  neutral /Li cell stored under open circuit conditions at  $95^\circ\text{C}$ . The values of the total interfacial resistance,  $R_i$ , and of its components, i.e. the passivation film resistance,  $R_f$  and the charge transfer resistance,  $R_{ct}$ , have been evaluated by fitting the impedance experimental results.

This is shown by Figures 2 and 3 which report the time evolution of three resistance terms in the two cases of cells based on neutral and acidic, respectively, electrolytes. The above mentioned resistance combination is clearly demonstrated.



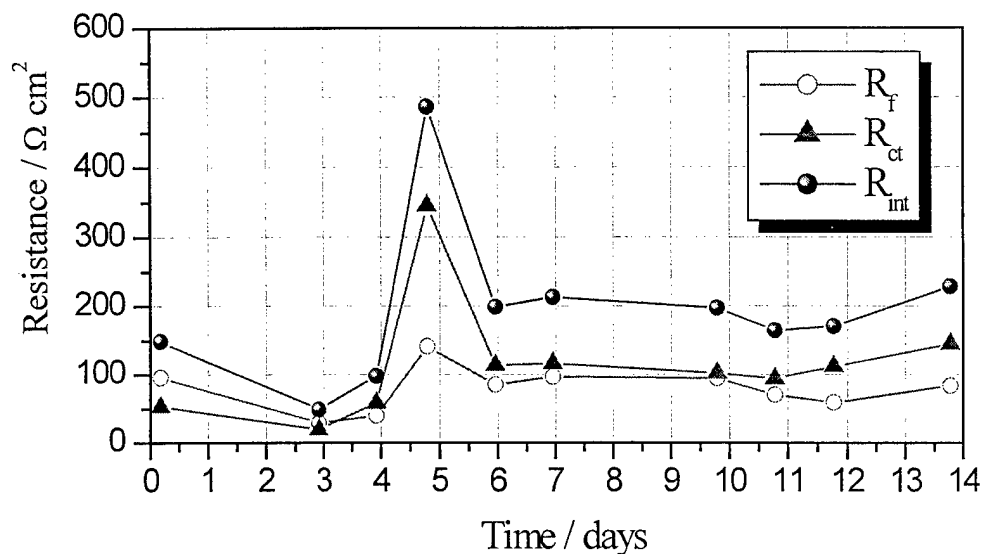


Figure 3. Time evolution of the resistance parameters of the  $\text{Li/P(EO)}_{20}\text{LiCF}_3\text{SO}_3 + 10 \text{ w/o Al}_2\text{O}_3 \text{ acid /Li}$  cell stored under open circuit conditions at  $95^\circ\text{C}$ . The values of the total interfacial resistance,  $R_i$ , and of its components, i.e. the passivation film resistance,  $R_f$  and the charge transfer resistance,  $R_{ct}$ , have been evaluated by fitting impedance experimental results.

By examining the trends of these figures one may notice that the resistance of the passivation film,  $R_f$ , after an initial rise, decreases and stabilizes at a low value for several days. This demonstrates that the passivation of lithium metal electrode is not a severe but rather a controlled effect in the composite polymer electrolytes here investigated. Since is the extent of this passivation that affects the cyclability of the electrode, it is possible to conclude that the three,  $\text{Al}_2\text{O}_3$ -based,  $\text{Li/P(EO)}_{20}\text{LiCF}_3\text{SO}_3$  nanocomposite are indeed suitable polymer electrolyte media for the development of stable and efficient rechargeable Li batteries. However, by comparing their specific properties in terms of ionic conductivity, lithium ion transference number, electrochemical stability window and lithium interface stability, the member of the family that appears to be the most promising for battery application is the  $\text{Li/P(EO)}_{20}\text{LiCF}_3\text{SO}_3 + 10 \text{ w/o Al}_2\text{O}_3$  neutral, composite polymer electrolyte.

Therefore, this composite was selected as the preferred electrolyte for exploiting its application as separator in novel types of rechargeable lithium batteries.

### Li- LiMn<sub>3</sub>O<sub>6</sub> polymer batteries.

Figure 4 shows a typical low-rate (C/40) discharge curve of the Li / P(EO)<sub>20</sub>LiCF<sub>3</sub>SO<sub>3</sub> +10 w/o neutral Al<sub>2</sub>O<sub>3</sub> / LiMn<sub>3</sub>O<sub>6</sub> battery at 105 °C. This quasi-thermodynamic curve evidences two voltage regions, to which one may tentatively associate the following processes:

Region 1, between 3.0 and 2.0 V, main reversible process:



to which is associated a maximum theoretical capacity of 210 mAh/g.

Region 2, below 2V, process of uncertain nature that leads to the irreversible formation of a spinel phase with consequent degradation of the cell performance. Therefore, it is recommended that the charge-discharge limits of the Li / P(EO)<sub>20</sub>LiCF<sub>3</sub>SO<sub>3</sub> +10 w/o neutral Al<sub>2</sub>O<sub>3</sub> / LiMn<sub>3</sub>O<sub>6</sub> battery are restricted between 3.5 V and 2.5V.

Assuming an average voltage of 3V, one derives a value of about 620 Whkg<sup>-1</sup> as the theoretical energy density of the Li / LiMn<sub>3</sub>O<sub>6</sub> polymer battery.

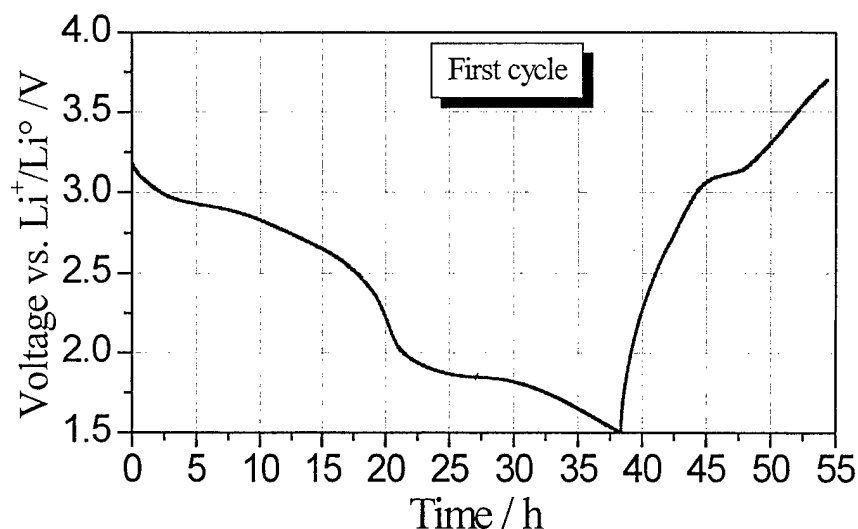


Figure 4. Voltage versus time profile of a low- rate, galvanostatic discharge of the Li / P(EO)<sub>20</sub>LiCF<sub>3</sub>SO<sub>3</sub> +10 w/o neutral Al<sub>2</sub>O<sub>3</sub> / LiMn<sub>3</sub>O<sub>6</sub> polymer battery at 105°C and in the 3.7 V – 1.5 V voltage window. The discharge curve is followed by a medium rate charge.

### Electrolyte stability window.

Figure 5 reports the capacity delivered by the battery under progressively higher discharge rates. The trend of the curves demonstrates that under the adopted configuration (i.e., source of cathode material and film electrode formulation) the cathode capacity rapidly decays from the 210 mAhg<sup>-1</sup> at C/40 to 170 mAhg<sup>-1</sup> at C/20, this initial decay likely being associated to diffusion polarization in the cathode. Then the capacity decays more smoothly from 170 mAhg<sup>-1</sup> to 120 mAhg<sup>-1</sup> passing from C/20 to C/4 rate. This second region may be associated to ohmic polarization. Finally, from C/4 to 3C the battery enters in the limiting current third region, this being associated to diffusion polarization in the electrolyte.

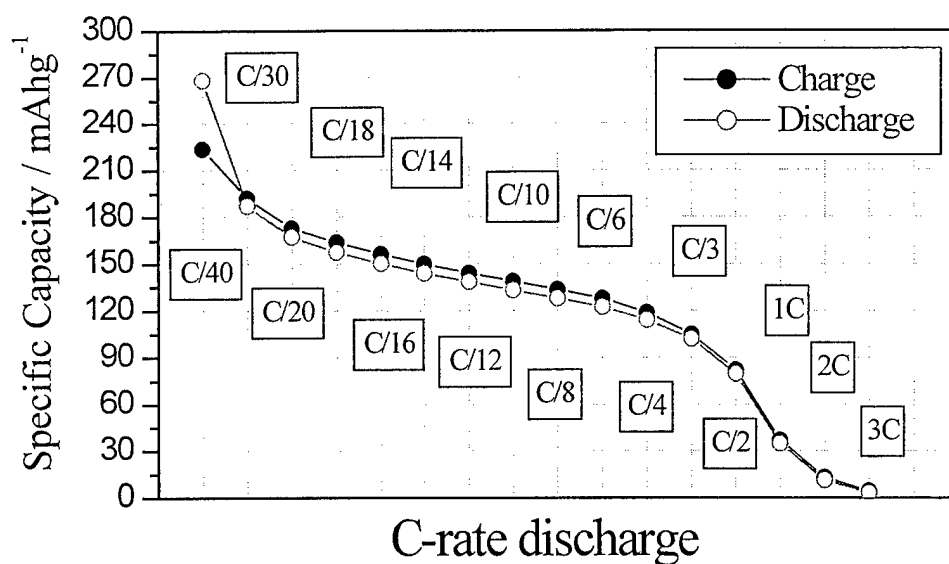


Figure 5. Capacity versus discharge rate of the Li / P(EO)<sub>20</sub>LiCF<sub>3</sub>SO<sub>3</sub> +10 w/o neutral Al<sub>2</sub>O<sub>3</sub> / LiMn<sub>3</sub>O<sub>6</sub> polymer battery at 105°C. Charge rate: C/10. Voltage window: 3.7 V – 1.5 V. Cathode source: US Army, Fort Monmouth.

These results suggest that the power capabilities of the battery may be improved in regions 1 and 2 by the optimization of: i) the  $\text{LiMn}_3\text{O}_6$  active compound by improving its chemical (purity) and morphological (particle size) properties and ii) the cathode film by improving the blending procedure and the reciprocal ratio between blend components (i.e., active material, binder and carbon additive).

Figure 6 shows the capacity delivery upon cycling of the Li /  $\text{P}(\text{EO})_{20}\text{LiCF}_3\text{SO}_3 + 10 \text{ w/o neutral Al}_2\text{O}_3 / \text{LiMn}_3\text{O}_6$  battery at  $105^\circ\text{C}$ . It may be seen that the cathode capacity constantly decreases upon cycling; however, the charge-discharge efficiency always approaches 100 %. This suggests that part of the active material is lost upon cycling, this being due either to  $\text{LiMn}_3\text{O}_6$  particle isolation in the electrode film structure and / or to increasing diffusion problems within the bulk of the particles.

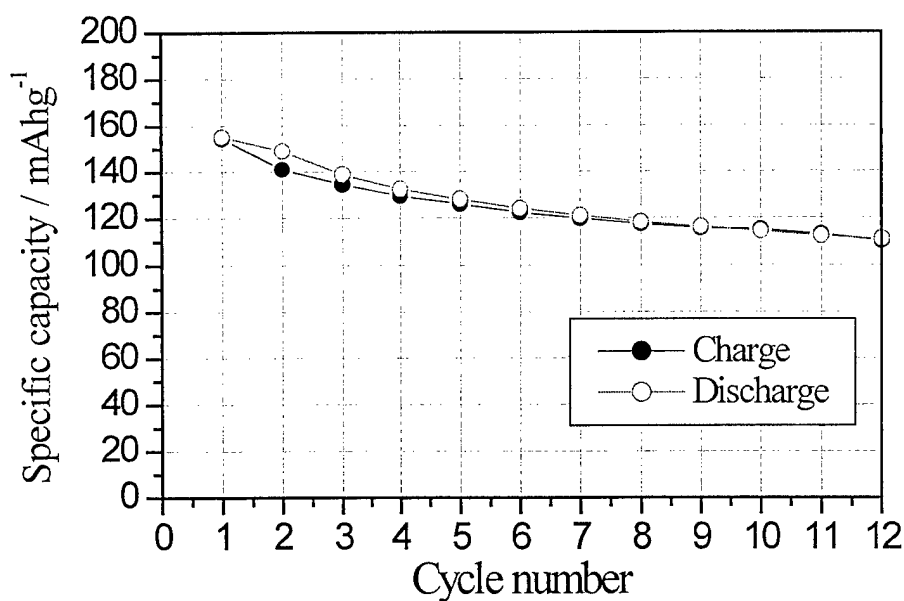


Figure 6. Capacity delivery upon cycling of the Li /  $\text{P}(\text{EO})_{20}\text{LiCF}_3\text{SO}_3 + 10 \text{ w/o neutral Al}_2\text{O}_3 / \text{LiMn}_3\text{O}_6$  polymer battery at  $105^\circ\text{C}$ . Charge-discharge rate: C/10. Voltage window: 3.7 V – 1.5 V. The discharge was run in the galvanostatic mode and the charge in the mixed galvanostatic – potentiostatic mode. Cathode source: US Army, Fort Monmouth.

These being the cases, the response of the battery is expected to improve following morphological optimization of the electrode formulation (e.g., reduction of  $\text{LiMn}_3\text{O}_6$  particle size, homogenization of the blend, choice of the most appropriate binder, ....)

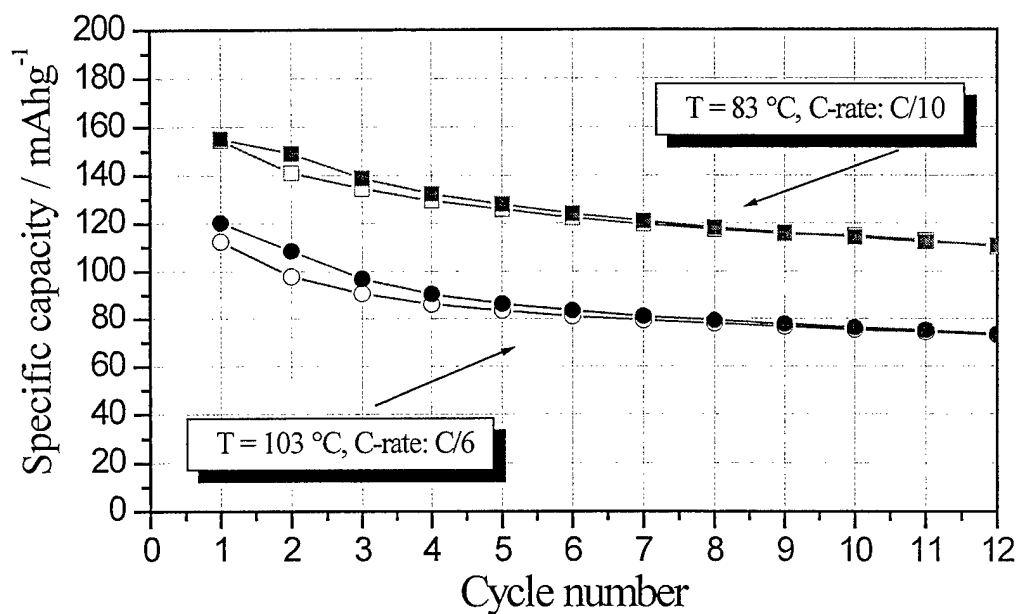


Figure 7. Comparison between the capacity delivery (lower panel) of the Li /  $\text{P}(\text{EO})_{20}\text{LiCF}_3\text{SO}_3 + 10$  w/o neutral  $\text{Al}_2\text{O}_3$  /  $\text{LiMn}_3\text{O}_6$  polymer battery cycled at 83°C and at 103 °C. Charge-discharge rate: C/10. Voltage window: 3.7 V – 1.5 V. Cathode source: US Army, Fort Monmouth.

Considering the improved transport properties of the composite polymer electrolyte used in this project the response of the battery was also investigated at medium-low temperatures. Figure 7 compares of the capacity delivery upon cycling obtained at 83 °C with those obtained at 103°C. Considering the difference in rate (C/10 for the test at 83°C and C/6 for the test at 103 °C), the

responses at the two temperatures are comparable. This in turn leads to conclude the following.

- i) The battery can operate at medium-low temperature, this confirming that the enhanced transport properties of the composite polymer electrolyte here used indeed allows operation temperature lower than those normally required for lithium polymer batteries based on conventional, ceramic-free, polymer electrolytes;
- ii) The decay in capacity upon cycling cannot be solely due to diffusion limitations within the bulk of the  $\text{LiMn}_3\text{O}_6$  cathode material since no substantial differences are found by varying the temperature of operation. Therefore, the decay may be more reasonably ascribed to deterioration of the electrode film structure (e.g., contact losses within particles) and / or of the single  $\text{LiMn}_3\text{O}_6$  particles (e.g., fractures). These effects may be contrasted by the choice of a more suitable binder and / or by the optimization of the  $\text{LiMn}_3\text{O}_6$  material.

To verify the above previsions, we have tested the response of batteries using alternative  $\text{LiMn}_3\text{O}_6$  cathode samples (kindly provided by Chunco Denki Koygo Co. LTD) and, to evaluate the role of the binder, we have prepared the film electrode replacing the PVdF with PEO.

Figure 8 shows the charge- discharge voltage profiles (upper panel) and the capacity delivery upon cycling of the battery using this new cathode source. The improvement in both cycling behavior and capacity delivery upon cycling is clearly shown. In addition, this highly favorable response is obtained at a temperature, i.e. 70 °C, even lower than that previously used. All this further supports the critical importance of selecting the proper electrolyte (e.g. composites) material and the most adequate electrode formulation (e.g. pure active compound and compatible binder) in view of assuring efficient performance of PEO-based lithium polymer batteries.

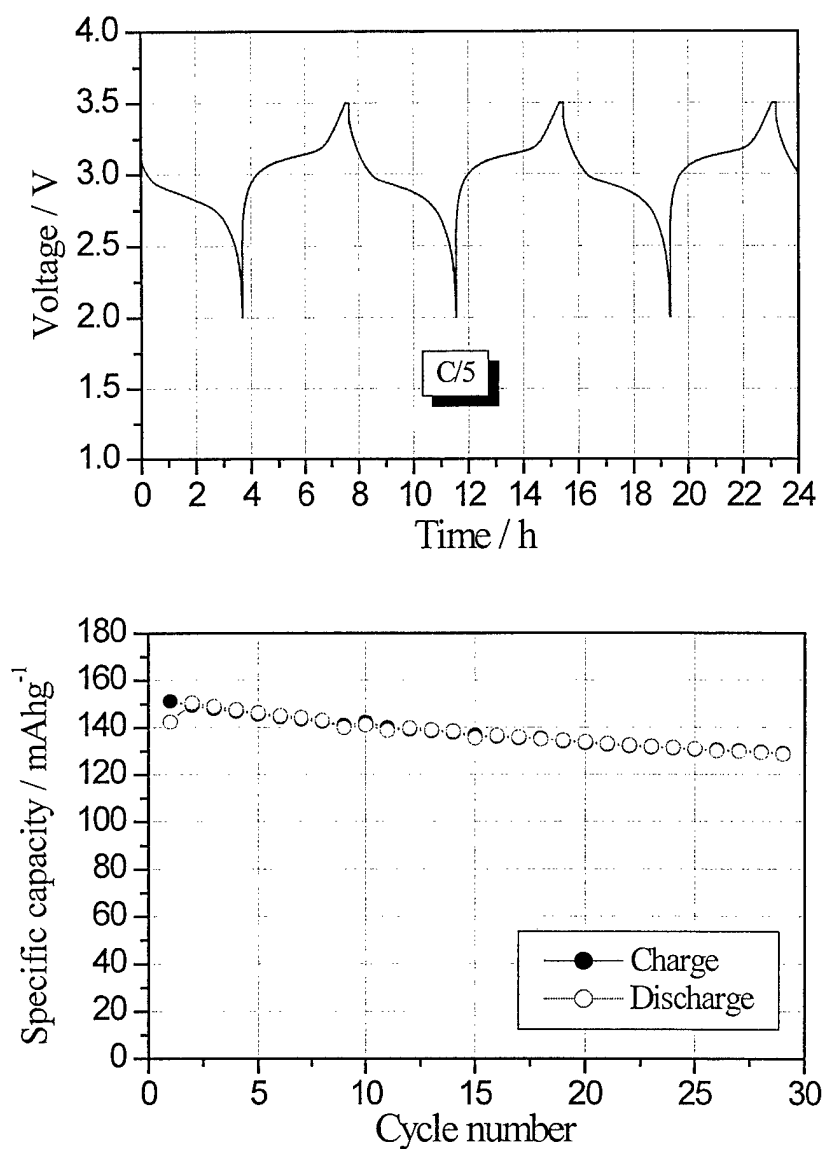


Figure 8. Voltage profiles (upper panel) and capacity delivery (lower panel) of the Li / P(EO)<sub>20</sub>LiCF<sub>3</sub>SO<sub>3</sub> +10 w/o neutral Al<sub>2</sub>O<sub>3</sub> / LiMn<sub>3</sub>O<sub>6</sub> polymer battery cycled 70 °C. Charge-discharge rate: C/5. Voltage window: 3.5 V – 2 V. Cathode composition: 80 wt% LiMn<sub>3</sub>O<sub>6</sub>, 10 wt% PEO (M.W. 4 000 000), 10 wt% Super P. Current density: 71 μAcm<sup>-2</sup>. T = 70°C. Cathode source: Chunco Denki Kogyo Co. LTD.

Finally, Figure 9 demonstrates that the battery may cycle very efficiently also at reasonably high rates at 70 °C, i.e. a temperature at which battery based on standard, ceramic-free polymer electrolytes are unable to operate.

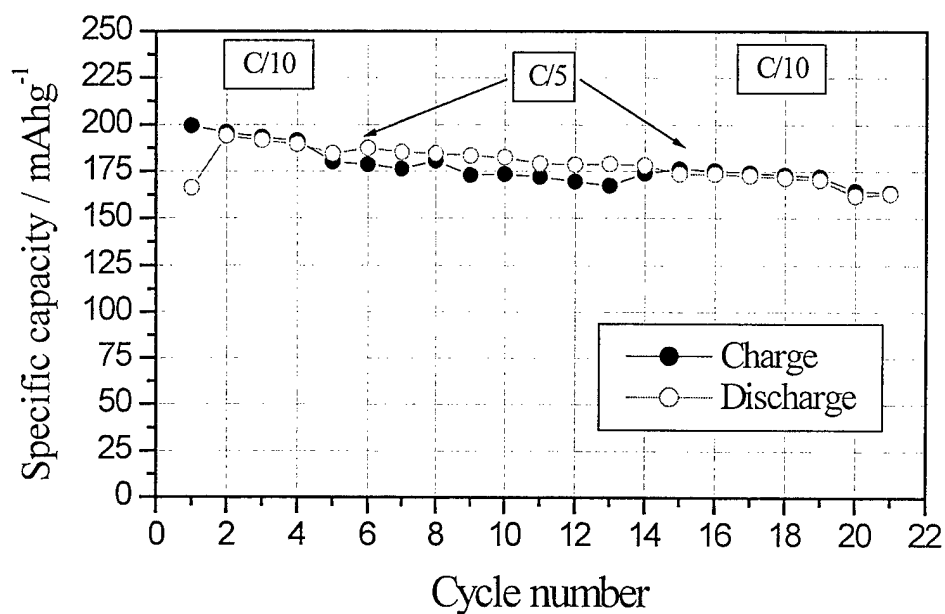


Figure 9 Capacity delivery upon cycling of the Li / P(EO)<sub>20</sub>LiCF<sub>3</sub>SO<sub>3</sub> +10 w/o neutral Al<sub>2</sub>O<sub>3</sub> / LiMn<sub>3</sub>O<sub>6</sub> polymer battery at 70°C. Charge-discharge rate: C/10. Voltage window: 3.5 V – 2.0 V. The discharge was run in the galvanostatic mode and the charge in the mixed galvanostatic – potentiostatic mode.



## 7. Conclusion

The results obtained in this project confirm that the overall properties of the  $\text{Li/P(EO)}_{20}\text{LiCF}_3\text{SO}_3 + 10 \text{ w/o Al}_2\text{O}_3$  composites are favorable for exploiting its application as polymer electrolyte separator in novel types of rechargeable lithium batteries capable of operating at medium low temperatures. In particular, the response of the prototypes fabricated and tested in the course of this project have demonstrated that the  $\text{LiMn}_3\text{O}_6$  compound is a cathode basically compatible with this electrolyte. However, the results

obtained under various experimental conditions also demonstrate that the electrochemical behavior of this compound is considerably dependent on the condition of its synthesis to the point that materials from different sources may give quite different responses. In addition, we have shown that the electrode formulation is also critical in assuring proper battery performance.

All this considering, we propose that the future work on this type of batteries should be directed along the following lines.

- i) Optimization of the synthesis conditions of the  $\text{LiMn}_3\text{O}_6$  cathode material.
- ii) Selection of alternative cathode materials have more stable structural retention upon cycling and capable to be prepared by a more straightforward and reproducible synthesis than  $\text{LiMn}_3\text{O}_6$ .
- iii) Optimization of the electrode film formulation, especially in terms of the choice of the most suitable binder and of the most appropriate composition ratio of the film blend.

AD NUMBER	DATE	DTIC ACCESSION NOTICE
1. REPORT IDENTIFYING INFORMATION		<b>REQU</b> 1. Put y on rei 2. Comp. 3. Attach maille 4. Use u infor. 5. Do no for 6  <b>DTIC:</b> 1. Asslg 2. Retu.  <b>20010827 066</b>
A. ORIGINATING AGENCY University of Rome, Italy		
B. REPORT TITLE AND/OR NUMBER Application of Composite Polymer Electrolytes		
C. MONITOR REPORT NUMBER R&D 8931-CH-01		
D. PREPARED UNDER CONTRACT NUMBER N68171-00-M-5848		
2. DISTRIBUTION STATEMENT  APPROVED FOR PUBLIC RELEASE  DISTRIBUTION UNLIMITED  FINAL		

DT.

OCT 95

EDITIONS ARE OBSOLETE